

# Synchronization of Traveling Waves within a Hollow-Core Vortex

H. Ait Abderrahmane, M. Fayed, H. D. Ng, G. H. Vatistas

**Abstract**—The present paper expands details and confirms the transition mechanism between two subsequent polygonal patterns of the hollow-core vortex. Using power spectral analysis, we confirm in this work that the transition from any  $N$ -gon to  $(N+1)$ -gon pattern observed within a hollow-core vortex of shallow rotating flows occurs in two steps. The regime was quasi-periodic before the frequencies lock (synchronization). The ratios of locking frequencies were found to be equal to  $(N-1)/N$ .

**Keywords**—Patterns, quasi-periodic, swirling, synchronization, transition.

## I. INTRODUCTION

SWIRLING flows produced in closed or open stationary cylindrical containers are considered as laboratory model for rotating flows encountered in nature and industries. These laboratory flows exhibit patterns similar to those observed in geophysical, astrophysical, and industrial flows. Three parameters, namely the initial fluid height and the disk speed and diameter, control the dynamics and the stability of such fluid motion which involves a solid-like body rotation and a shear layer flow. Because of the cylindrical confining wall, the bulk flow is formed by two distinct flow regions, namely the shear layer and solid-like body rotation flows. The former flow occupies the outer region around the walls; it surrounds the second flow, which occupies the inner region. The interface between these two flows is subject to Kelvin-Helmholtz instability. This instability manifests as azimuthal waves which roll up into satellite vortices and in turn impart the interface polygonal shapes, e.g. see [3], [4], [6]-[8]. The inner solid-like body rotation region can also be subjected to inertial instabilities which manifest as Kelvin's waves. The rotating wave observed in our experiments belongs to this type of waves. Indeed, in our experiment, a hollow-core vortex, produced by a rotating disk near the bottom of a vertical stationary cylinder, is within the inner solid body rotation flow region and acts as a wave guide to azimuthal rotating Kelvin's waves. First, the shape of hollow-core vortex was circular before it bifurcates into rotating waves (polygonal patterns), when a critical disk speed was reached, the maximum wave

number observed is the hexagon.

Since the instability mechanisms at work in our experiment and in other studies such as [7] are different, one should expect that the results of the variation of the control parameters will be different. Indeed, in the experiment carried by Poncet and Chauve [7], increase in the disk speed results in the increases of the shear; as a consequence, the satellite vortices merge and their number decreases. This explains the decrease of the number of the sides of the polygonal patterns in their experiment. However, in our experiment the number of the sides of the polygonal pattern increases with the disk speed; this can be interpreted as an increase in the vibrating mode of a system to the increase of input energy due to the disk rotation. Moreover, the mechanisms leading to the transition between polygonal patterns are also different in our experiment and those of Chomaz et al. [3]. In the latter, the patterns are caused by Kelvin-Helmholtz instability. Chomaz et al. [3] reported that the leading mechanism, that governs the transition from one pattern to another when the disk speed was increased, is the well known sub-harmonics cascade. However, in our experiments the transition from  $N$ -gon to  $(N+1)$ -gon was found to follow another route; it occurs through synchronization of the two rotating waves with wave numbers  $N$  and  $N+1$ . This transition was previously proposed and partially described in Ait Abderrahmane et al. [1] using the nonlinear dynamics theory. The latter was built on the observation of one transition, from 3-gon to 4-gon. In the present paper, other transitions are analyzed to establish the transition mechanism from  $N$ -gon to  $(N+1)$ -gon.

## II. EXPERIMENTAL SETUP AND MEASUREMENT TECHNIQUE

### A. Experimental Setup

As shown in Fig. 1, a stationary cylindrical container was used with 284 mm diameter. The rotating disk with 252 mm diameter was fixed at 20 mm from the bottom. The experiment was conducted for two initial water heights, 20 mm and 40 mm. Our experiments are similar to those conducted by Jansson et al. [5]. They used similar setup with different dimensions. Similar phenomenon polygonal patterns at the surface of the disk were observed in both experiments. The disk was coated with white plastic sheet for better visualization; however, it does not influence prominently the transition mechanism.

H. Ait Abderrahmane is with the Department of Mechanical and Materials Engineering, Masdar Institute, Abu Dhabi, United Arab of Emirates (phone: +971 2 810 9306, e-mail: haitabd@hotmail.com).

M. Fayed is with Mechanical Engineering Department, College of Engineering and Technology American University of The Middle East Kuwait and Mechanical Engineering Department, Alexandria University, Alexandria, Egypt (e-mail: Mohamed.fayed@aum.edu.kw).

H. D. Ng and G. H. Vatistas are with Department of Mechanical and Industrial Engineering, Concordia University, Montreal, Quebec, H3G 1M8, Canada (e-mail: hoing@encs.concordia.ca, vatistas@encs.concordia.ca).

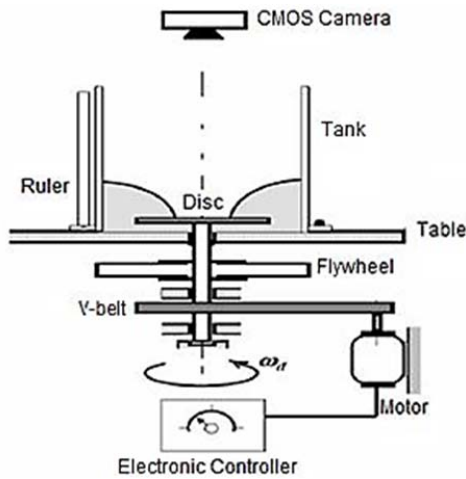


Fig. 1 Experimental setup

The rotation of the circular disk at the bottom of the tank introduces angular momentum into the flow. This angular momentum is directed towards the cylindrical wall by the radial velocity component. Cylindrical wall diverts this flow towards the interior, and a meridional overturning flow is established. As the rotating frequency of the disc increases, the meridional flow imparts enough angular momentum towards the cylinder axis to establish a central vortex flow. With a further increase in the disc frequency, the magnitude of angular momentum directed towards the central axis increases, and the flow balances this angular momentum by an increased radial flow outwards from the central axis. This radial outflow causes a pressure reduction in the central region. As the radial outflow becomes sufficiently strong, a depression is generated in the central region and the water free surface first takes a shape of inverted bell and then forms a hollow core-vortex when the speed of rotating disk reaches a critical value. As the free surface touches the surface of the disk, the line intersection between the liquid and the surface of disk outlines the core shape. The resulting hollow-core vortex is characterized by a thin layer of fluid in solid-like body rotation; this layer surrounds the hollow. This layer is also surrounded by a shear flow region where the azimuthal velocity decreases in the radial direction until it vanishes at the wall of the container. The shape of the hollow or the inner solid-like body rotation layer changes with the disk speed. As the speed of the disk increases, the circular shape of the core first becomes elliptical and then acquires different polygonal shapes; see Fig. 2. It is worth noting that the apexes of the resulting polygonal patterns are located on almost invariable circle of radius approximately half the tank radius.

Three parameters determine generally the formation of the patterns and their stability; namely, the water height, speed and radius of the disk. The variation of any of these parameters has a consequence on pattern formation and its transition towards a nearby pattern. For instance, increasing the water height causes a transition from  $(N+1)$ -gon and  $(N)$ -gon while decreasing the water height produces a transition from  $(N+1)$ -gon into  $(N)$ -gon. Similarly, increasing the disk

radius produces a transition from  $(N+1)$ -gon into  $(N)$ -gon, and the transition occurs in the opposite direction when the disk speed is decreased. However, in our studies, we have chosen to vary the disk speed because it is more practical and consistent to control for a wide range of variation.

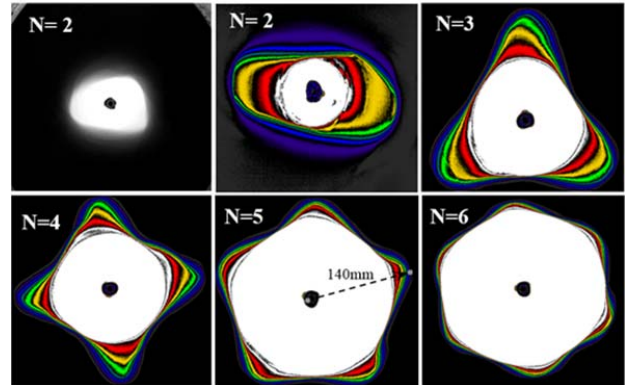


Fig. 2 Polygonal vortex-core patterns. The inner white region is the dry part of the disk. The colors indicate the variation of water depth from the inner to the outer flow region

While the mechanism leading to the formation of the hollow vortex-core is basically understood, the physics behind the formation of the patterns remains unclear. Swirling flows such as ours are subject to the influence of three instability mechanisms: inertial, Kelvin-Helmholtz, and centrifugal instabilities. In very shallow water condition, the prominent instability mechanism behind the formation of the polygonal pattern appears to be Kelvin-Helmholtz. This mechanism is at work at the interface between the inner solid-like body rotation and the shear flow regions. However, when the water height is higher but sufficiently small to satisfy a shallow water condition, the instability mechanism at work turns to be inertial instability. This mechanism is at work in solid-like body rotation flow region such as vortex cores. According to vortex stability theory, such instability mechanism leads to the formation of Kelvin's waves. In our experiment, the patterns occur in the inner region, i.e. in the solid-like body rotation, which is more prone to inertial instability. However, in both cases of very shallow and shallow water condition, both mechanisms should be at work even one of them dominates in one or other cases. Moreover, because of the momentum stratification in the radial direction, the centrifugal instability mechanism should also play a role. The interplay of these three instability mechanisms during the formation and their stability remains unclear. A thorough theory that can explain the formation such patterns and the interaction the different instabilities needs to be developed; experimental results like the ones reported in the present study can help in developing of theory that might shed light on the physics of this phenomenon.

For exceedingly low rotational disk speeds ( $f_d$ ), the vortex core remains circular ( $N= 0$ ). Increasing its rotation, the hollow-vortex core starts to wobble ( $N= 1$ ). A further increase of disk speed yields progressively the vortex-core to

“elliptical” ( $N= 2$ ), triangular ( $N= 3$ ), square ( $N= 4$ ), pentagonal ( $N= 5$ ), and hexagonal ( $N= 6$ ) patterns as illustrated in Fig. 2. To increase the visibility of the patterns, a blue water-soluble dye was injected into the water and uniform circular lighting was used. A CMOS high-speed camera (pco.1200hs) was placed on the top of the cylinder, and the hollow-vortex core formed on the disk was imaged. The camera acquired sequence of images at a rate of 30 frames per second with an exposure time of 1/510 second. The colored images illustrate the stratification of the hollow-core vortex. Each color indicates a water depth within the vortex core, which increases continuously as we move away from the center of the disk. The continuous increase in the water depth, depicted in the Fig. 2 by the colored layers indicates momentum stratification in the radial direction. Moreover, Fig. 2 indicates the shrinking of the inner solid-like body rotation flow region as we move ahead towards higher modes. This indicates the interpenetration of the outer shear layer flow region into the inner one. The prominence of the shear flow at higher modes and the disappearance of the solid-like flow region in favor of the shear flow region might explain the limited number of instability modes. The instability modes are tightly related to the inertial instability acting in the inner solid-like rotation region and they are limited to six (hexagonal pattern); see Jansson et al. [5] and Vatistas et al. [9]. For the quantitative analysis, we used the grey images.

### B. Measurement Technique

The transition is investigated using image processing technique. First, the original 8-bit gray-scale image is converted into a binary image, using a suitable threshold, in order to extract the polygonal contours. A low low-pass Gaussian filter was applied to get rid of the remaining image noises. The standard edgetection procedure was used to get the boundaries of the pattern.

### III. RESULTS AND DISCUSSION

We use the Fast Fourier Transform (FFT) analyze of the time series of the radial displacement for a given point on the contour. At the beginning, the disk speed is fixed at  $f_d = 2.3$  Hz, the hollow-core espouses an ellipse ( $N= 2$ ) revolving with a frequency  $f_p = 0.73$  Hz which is half of the fundamental frequency  $f_l = 1.46$  Hz, the frequency of the mode of higher amplitude; see Fig. 3. Increasing gradually the speed of the disk, the ellipse opens up, and its contours become distorted by a growing wave ( $N= 3$ ). Increasing further the frequency of the rotating disk up to  $f_d = 3.08$  Hz, the pattern undergoes a transition from a distorted ellipse to a triangular shape ( $N= 3$ ). The power spectrum that corresponds to this transition is shown in Fig. 4. The power spectrum shows that during the transition process, the amplitude of the modulating wave  $N= 3$  is of the same order as of the initial pattern,  $N= 2$ . The two frequencies are irrefutably present; they are respectively  $f_1 = 1.64$  Hz and  $f_2 = 3.19$  Hz. The ratio,  $f_1/f_2$ , between these two frequencies is approximately equal to  $1/2$ , which indicates that the transition occurs when the two waves lock or synchronize. This frequency locking is consistent with the theory of stability of quasi-periodic regimes, see [2]. Increasing further the disk speed to  $f_d = 3.1$  Hz, the transition is completed and the vortex-core shape set in  $N= 3$  pattern; the power spectrum shown in Fig. 5 displays clearly the  $N= 3$  fundamental frequency  $f_l = 3.2$  Hz. Continuing the increase of the disk speed, the triangular pattern was brought towards the transition into square pattern. Similar to the first transition from elliptical to triangular core, at a certain critical disk speed, the modulating wave  $N= 4$  synchronizes with the triangular wave ( $N= 3$ ) and the transition occurs; this critical speed is found to be  $f_d = 3.51$  Hz. The power spectrum corresponding to this transition is shown in Fig. 6. The figure shows two frequencies  $f_1 = 3.2$  Hz and  $f_2 = 4.71$  Hz that correspond to the patterns  $N= 3$  and  $N= 4$ , respectively. The ratio between these two frequencies is very close to  $2/3$ . At slightly higher disk speed  $f_d = 3.55$  Hz, the square pattern sets in; see Fig. 7. Increasing further the disk speed, the square pattern undergoes a transition into a pentagon. The transition from  $N = 4$  to  $N = 5$  occurs at disk speed of  $f_d = 3.8$  Hz; similarly to previous transitions, the power spectrum indicates the presence of two dominant frequencies  $f_1 = 4.75$  Hz and  $f_2 = 6.01$  Hz (as shown in Fig. 8). The ratio between these two frequencies is very close to  $4/5$ . Increasing slightly the disc speed, the pattern becomes a pentagon. Fig. 9 shows the power spectrum for this pentagon pattern where the fundamental frequency is  $f_l = 6.1$  Hz. Because the disk speed interval

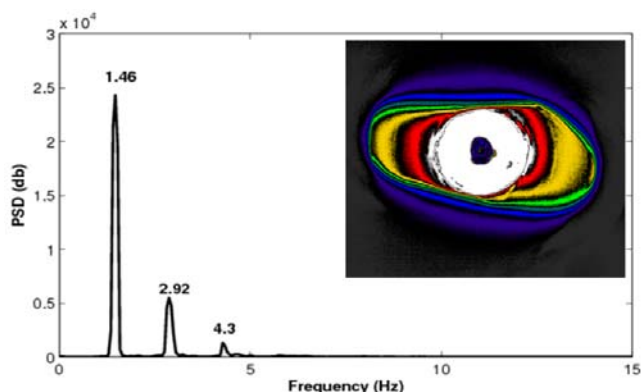


Fig. 3 Elliptical pattern ( $N= 2$ ) and corresponding power spectrum

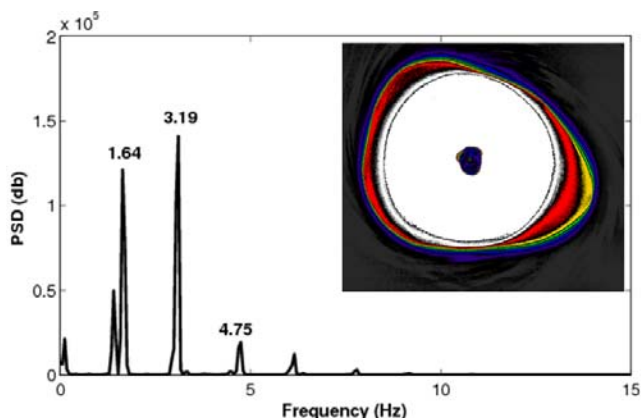


Fig. 4 First transition from  $N=2$  to  $N=3$  and corresponding power spectrum

where the pentagon occurs was so narrow that it was impossible for us to follow the transition towards the hexagon and perform proper power spectrum analysis. However, based on the previous observations, we can anticipate that it would follow the same route behavior, i.e. the transition will occur when the wave  $N=6$  synchronize with the wave  $N=5$  and the ratio between the frequencies is close to  $5/6$  dimensionally.

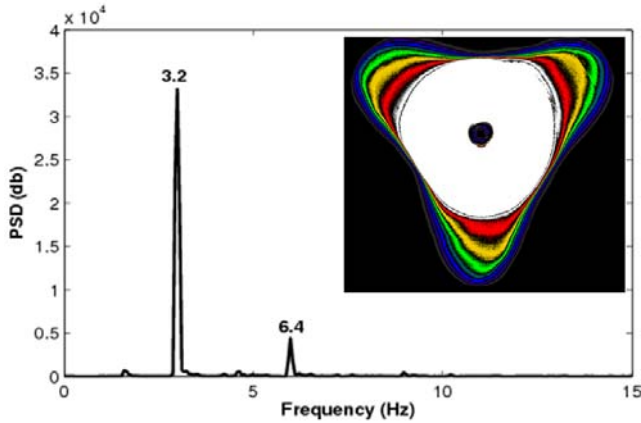


Fig. 5 Triangular pattern ( $N = 3$ ) and corresponding power spectrum

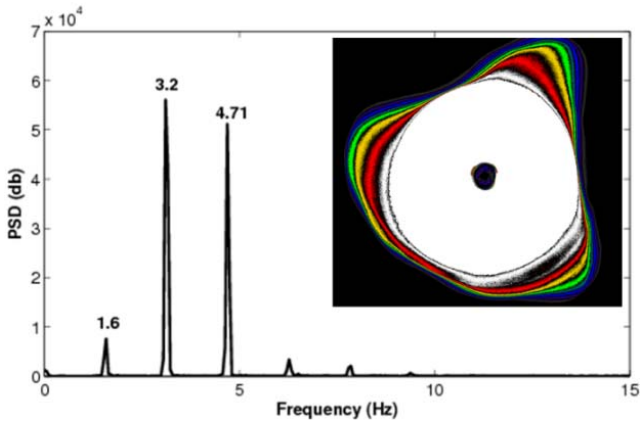


Fig. 6 Second transition from  $N=3$  to  $N=4$  and corresponding power spectrum

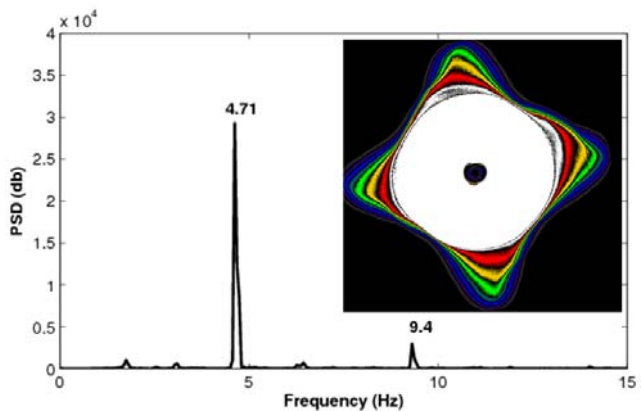


Fig. 7 Square pattern ( $N = 4$ ) and corresponding power spectrum

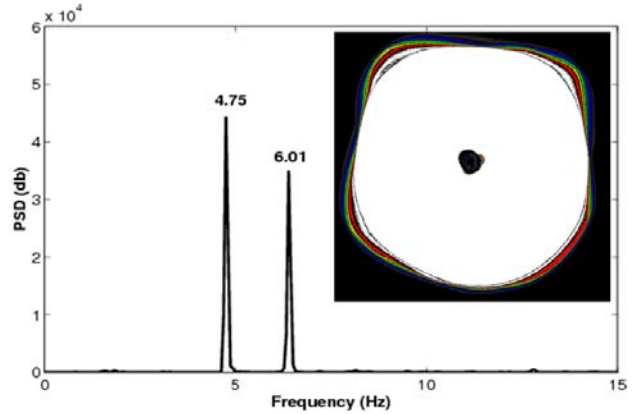


Fig. 8 Third transition from  $N=4$  to  $N=5$  and corresponding power spectrum

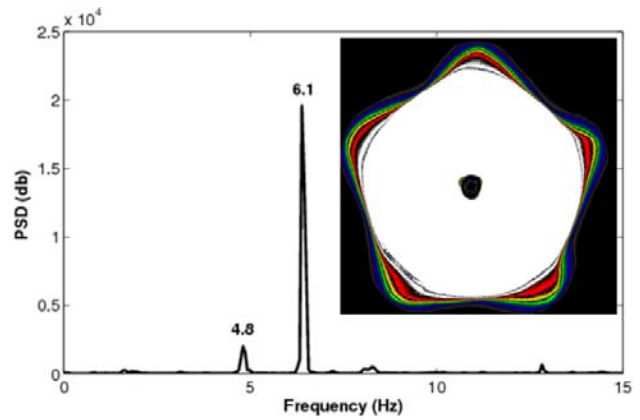


Fig. 9 Pentagonal pattern ( $N = 5$ ) and corresponding power spectrum

#### IV. CONCLUSION

Through the present experiments, we confirmed the transition mechanism between two subsequent polygonal waves patterns, observed within the hollow-core vortex of shallow rotating flows. The transition involves the universal route of quasi-periodic regime and synchronization. The transition occurs when the frequencies corresponding to  $N$  and  $N+1$  waves lock at a ratio of  $(N-1)/N$ .

#### ACKNOWLEDGMENT

This work is supported by the Natural Sciences and Engineering Research Council of Canada (NSERC).

#### REFERENCES

- [1] H. Ait Abderrahmane, K. Siddiqui, and G. H. Vastias, "Transition between Kelvin's equilibria," *Phys. Rev. E*, 2009, no.80, 066305.
- [2] P. Bergé, Y. Pomeau, and C. Vidal, "Order Within Chaos," Hermann, Paris, 1984.
- [3] J. M. Chomaz, M. Rabaud, C. Basdevant, and Y. Couder, "Experimental and numerical investigation of a forced circular shear layer," *J. Fluid Mech.*, 1988, 187, pp. 115-140.
- [4] R. Hide, and C. W. Titman, "Detached shear layers in a rotating fluid." *J. Fluid Mech.*, 1967, vol. 29, pp. 39-60.
- [5] T. R. N. Jansson, M. P. Haspang, K. H. Jensen, P. Hersen, and T. Bohr, "Polygons on a rotating fluid surface," *Phys. Rev. Lett.*, 2006, no. 96.
- [6] H. Niino, and N. Misawa, "An experimental and theoretical study of barotropic instability." *J. Atmos. Sci.* 1984, vol. 41, pp. 1992-2011.

- [7] S. Poncet and M. P Chauve, "Shear-layer instability in a rotating system," *J. Flow Visualization and Image Processing*, 2007, no. 14 (1), pp. 85-105.
- [8] M. Rabaud, and Y. Couder, "Instability of an annular shear layer," *J. Fluid Mech.*, 1983, vol. 136, pp. 291–319.
- [9] G. H. Vatistas, H. Ait Abderrahmane, and K. Siddiqui, "An experimental confirmation of Kelvin's equilibria," *Phys. Rev. Lett.*, 2008, no. 100, 17450.